

# Fabrication of Angiogenic Sprouting Co-Culture of Cell Clusteroids by Using an Aqueous Two-Phase Pickering Emulsion System

Anheng Wang,<sup>a</sup> Leigh A. Madden,<sup>b</sup> and Vesselin N. Paunov<sup>\*,c</sup>

<sup>a</sup> Department of Chemistry and Biochemistry, University of Hull, Hull, HU67RX, U.K.

<sup>b</sup> Department of Biomedical Sciences, University of Hull, Hull, HU67RX, U.K.

<sup>c</sup> Department of Chemistry, Nazarbayev University, 53 Kabanbay Batyr Avenue, Nursultan city, 010000, Kazakhstan.

\* Corresponding author email: [vesselin.paunov@nu.edu.kz](mailto:vesselin.paunov@nu.edu.kz)

**KEYWORDS:** Co-culture; angiogenesis; aqueous two-phase system, water-in-water Pickering emulsion; 3D cell culture

**ABSTRACT:** Tumor cell spheroids and 3D cell culture has generated a lot of interest in the past decade due to their relative ease of production and biomedical research applications. To date, the frontier in tumor 3D models has been pushed to the level of personalized cancer treatment and customized tissue engineering applications. However, without vascularization, the central parts of these artificial constructs cannot survive without an adequate oxygen and nutrient supply. The formation of a necrotic core into *in-vitro* 3D cell models is still serving as the major obstacle in their wider practical application. Here we propose a rapid formation protocol based on using a water-in-water (w/w) Pickering emulsion template to generate a phenotypically endothelial/hepatic (ECV304/Hep-G2) co-culture cell clusteroids with angiogenic capability. The w/w Pickering emulsion template was based on a dextran/poly(ethylene oxide) aqueous two-phase system stabilized by whey protein particles. The initial cells proportion in the co-culture clusteroids can easily be manipulated for optimal performance. The co-cultured pattern of the endothelial/hepatic cells could significantly promote the production of angiogenesis-related proteins. Our study confirmed that co-cultured clusteroids can stimulate cell sprouting without the addition of vascular endothelial growth factor (VEGF) or other angiogenesis inducers at a ratio of 1:2 of Hep-G2: ECV 304. Angiogenesis genes production in the co-culture clusteroids was enhanced with VEGF, urea, IGFBP, along with angiogenesis-related marker CD34 levels also indicating angiogenesis progress. Our aqueous two-phase Pickering emulsion templates provided a convenient approach to vascularize a target cell type in 3D cell co-culture without additional stimulating factors, which could potentially apply to either cell lines or biopsy tissues, expanding the clusteroids downstream applications.

## INTRODUCTION

Compared with the traditional 2D culture, 3D cell culture tends to simulate the *in vivo* environment by confining the cells into densely packed aggregates to enhance cell-to-cell interaction and their functionality.<sup>1,2</sup> 3D cell culture models have recently garnered great attention because they often promote levels of cell differentiation and tissue organization, which are unachievable in conventional 2D culture.<sup>3,4</sup> The most used animal models generally require sophisticated operation and strict ethical review.<sup>5</sup> Due to this, animal experiments are still struggling to provide a reference for clinical trials.<sup>6</sup> The high availability and precise mimicry of real-life environments has drawn interest in the 3D cell culture models in the past decade. The most discussed 3D cell culture models, depending on the fabrication methods, are spheroids and organoid models.<sup>7</sup>

The cell spheroids are often used as a preclinical assessment model for the biological performance of various drugs or therapeutics.<sup>8,9</sup> Recently, there has been a trend to expand the application of spheroids into tissue engineering applications, which would utilize them as building blocks to reconstitute scaled artificial organs *in vitro*.<sup>10-12</sup> The artificial tissue could be used to replace or repair damaged organs, such as skin, bone, and others. Nevertheless, the reconstruction of living organs using 3D cell cultured models is still facing crucial interference, especially on multiple species cell-cell interfaces. Spatiotemporal gradients of chemicals and oxygen are key features in cell proliferation in spheroids.<sup>13</sup> Cell spheroids of nonendothelial cells will inevitably form necrotic cores where essential chemicals and oxygen cannot be delivered due to the absence of a vascular system. A high vascularization state of the spheroids is a crucial step before the spheroids can be systematically used since the cores of these artificial constructs cannot survive longer periods of culturing without this tubular network.

Angiogenesis is initiated by pro-angiogenic growth factors, such as vascular endothelial growth factor (VEGF).<sup>14,15</sup> These factors stimulate the conversion of endothelial cells from their resting stage into activated tip cells.<sup>16</sup> The tip cells degrade the extracellular matrix by releasing matrix metalloproteinases (MMPs) and migrate into the surrounding tissue or extracellular matrix (ECM) *in vitro*.<sup>17,18</sup> They are followed by proliferating endothelial stalk cells, resulting in the formation of capillary buds and sprouts, which progressively grow toward the angiogenic stimulus.<sup>19</sup> Finally, the sprouts form a lumen and interconnect with each other to new blood-perfused microvessels.<sup>20</sup> Endothelial cells (E.Cs.) spontaneously form a vascular-like network due to endothelial sprouting (angiogenesis) upon coculture with other cell types.<sup>21-23</sup> Recently, Correa de Sampaio et al.<sup>47</sup> reported a 3D model of the sprouting coculture of fibroblast and endothelial cells.

The hanging drop method was a previously reported coculture of fibroblasts and human umbilical vein endothelial cells (HU-VECs) to generate composite vascularized spheroids.<sup>24</sup> The fibroblasts were considered to impose a vascularization signal to the E.Cs., which would spontaneously generate a vascular network in the coculture spheroids. Mesenchymal stem cells and several tumor cells were also capable of stimulating the vascularization in the coculture pattern with E.Cs.<sup>25-27</sup> However, the microfluidic devices or extracellular matrixes used for coculturing spheroids were usually of a low yield rate or high labor cost, which greatly limited the practical application of the vascularized spheroids. Atefi et al.,<sup>28</sup> Lemmo et al.,<sup>29</sup> and Das et al.<sup>30</sup> developed a high throughput production method for a 3D cell clusteroid-based aqueous two-phase system (ATPS) as a water-in-water Pickering emulsion stabilized by  $\beta$ -lactoglobulin or whey protein particles. Several follow up reports have emerged after the method was first introduced, which indicate the increased functionality and high productivity of the generated clusteroids based on this novel approach.<sup>31-33</sup> The manufacturing process using water-in-water (w/w) Pickering emulsion as a template might potentially satisfy the requirements of high throughput and of cell coculture simultaneously. The collected 3D cell clusteroids differ from classical spheroids, as the former are of higher porosity and have no necrotic core as media can freely diffuse and reach the cores. The usage of coculturing cell lines with the help of this w/w Pickering emulsion system has not been reported before.

In this study, we systematically generated and characterized cocultured Hep-G2/ECV304 clusteroids using the w/w Pickering emulsion as a template (see Figure 1). The Hep-G2 cells were cocultured with ECV-304 cells to generate vascularized cocultured clusteroids on a large scale in a proof of principle study. In general, the cell types could be switched to any cell line or primary cell culture. The obtained cocultured clusteroids showed a significant increment in angiogenesis compared to the single clusteroids as reported below. We found that, especially at a cell ratio of Hep-G2/ECV304 of 1:2, the coculture clusteroids could spontaneously form sprouts after they were embedded into a supporting matrix of sodium alginate hydrogel. The high yield and the reproducibility of the method would make itself an ideal protocol for tissue engineering and advanced drug testing applications. This new facile platform has the potential to enhance the applications of coculture clusteroids

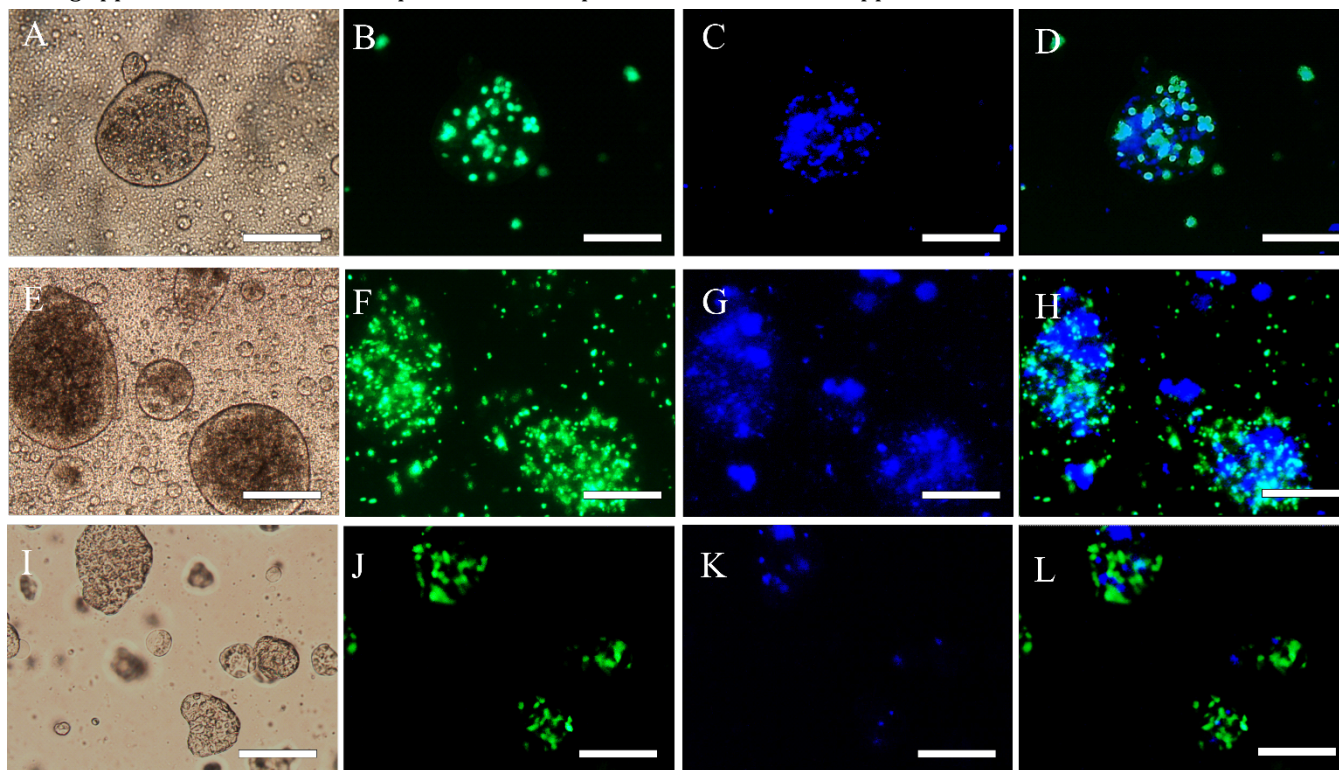


**Figure 2.** Bright-field (A, E, I) and fluorescence microscope observation of mixed Hep-G2/ECV 304 (cell ratio=1:1) cells encapsulated by 5.5 wt% DEX in 5.5 wt% PEO emulsions before (A-H) and after shrinking by 11 wt% PEO (I-L) set at FITC (B, F, J), DAPI (C, G, K)

and Dual fluorescence (D, H, L) channels. The Hep-G2 cells and ECV 304 cells were pre-stained with DAPI and CMFDA, respectively. The bar is 100  $\mu\text{m}$  for (A-D) and (I-L). The bar for (E-H) is 50  $\mu\text{m}$ .

## EXPERIMENTAL SECTION

### Materials

CellTracker™ Green CMFDA Dye, CFSE far-red, CFSE green fluorescence dye and cell culture 24-well plates were sourced from Thermo Fisher Scientific, UK. Dextran (DEX) (MW 500 kDa) and polyethylene oxide (PEO) (MW 200 kDa) were purchased from Sigma-Aldrich, UK. Sodium chloride (99.8%) and calcium chloride (99%), Dulbecco's Modified Eagle Medium, and Trypsin-EDTA were sourced from Fisher Scientific, UK. Media supplements were fetal bovine serum (10% v/v, Labtech, Heathfield, UK) and 0.25% Trypsin-EDTA (1X, Lonza). The ECV 304 and Hep-G2 cell line were purchased from ECACC cell collection. Urea analysis kit was obtained from Sigma Aldrich (Saint Louis, USA). The MMP-2 ELISA kit was sourced from GE healthcare (Amersham, UK), the IGFBP ELISA kit and angiogenesis array kit were sourced from the Bio-technie (Abingdon, UK). The urea kit was provided by Sigma-Aldrich, UK. Whey protein was kindly provided by No 1 Supplements (Suffolk, UK). Deionized water was purified by reverse osmosis and ion exchange with Milli-Q water system (Millipore, USA) was used in all our studies. Deionized water surface tension was 71.9  $\text{mN m}^{-1}$  at 25 °C, with resistivity higher than 18  $\text{M}\Omega \text{ cm}^{-1}$ . All the other chemicals are of analytical grade.

### Methods

#### ECV 304 and Hep-G2 monolayer cell culture

The human cell line ECV 304 is categorized as a T24 derivative (urinary bladder carcinoma), which was believed to originate from endothelial cells obtained from the umbilical vein of a healthy donor.<sup>33</sup> The ECV 304 cell line contains many important characteristics of endothelial cells. The immortalized nature of this cell line makes it a valuable model to set an initial model for endothelial vascularization.<sup>33</sup> The ECV 304 and Hep-G2 cell lines were cultured in DMEM and EMEM mediums, respectively, supplemented with 10 % Fetal Bovine Serum. Both types of cells were cultured in T75 easYFlask (Thermo Fisher Scientific, U.K.) at 37°C supplemented 5 %  $\text{CO}_2$ . The medium was discarded when the cells reached a confluency of 80% before the cells were rinsed with phosphate buffer saline (PBS, Lonza, UK) twice to remove the excessive medium. The cells were then detached from the flasks using 0.25 wt% trypsin solution and passage in 1:8 (ECV304) and 1:4 (Hep-G2). The trypsinization was stopped by mixing the trypsin solution with a proper complete medium (either DMEM or EMEM), and the cells were collected by centrifugation at 400×g for 4 min.

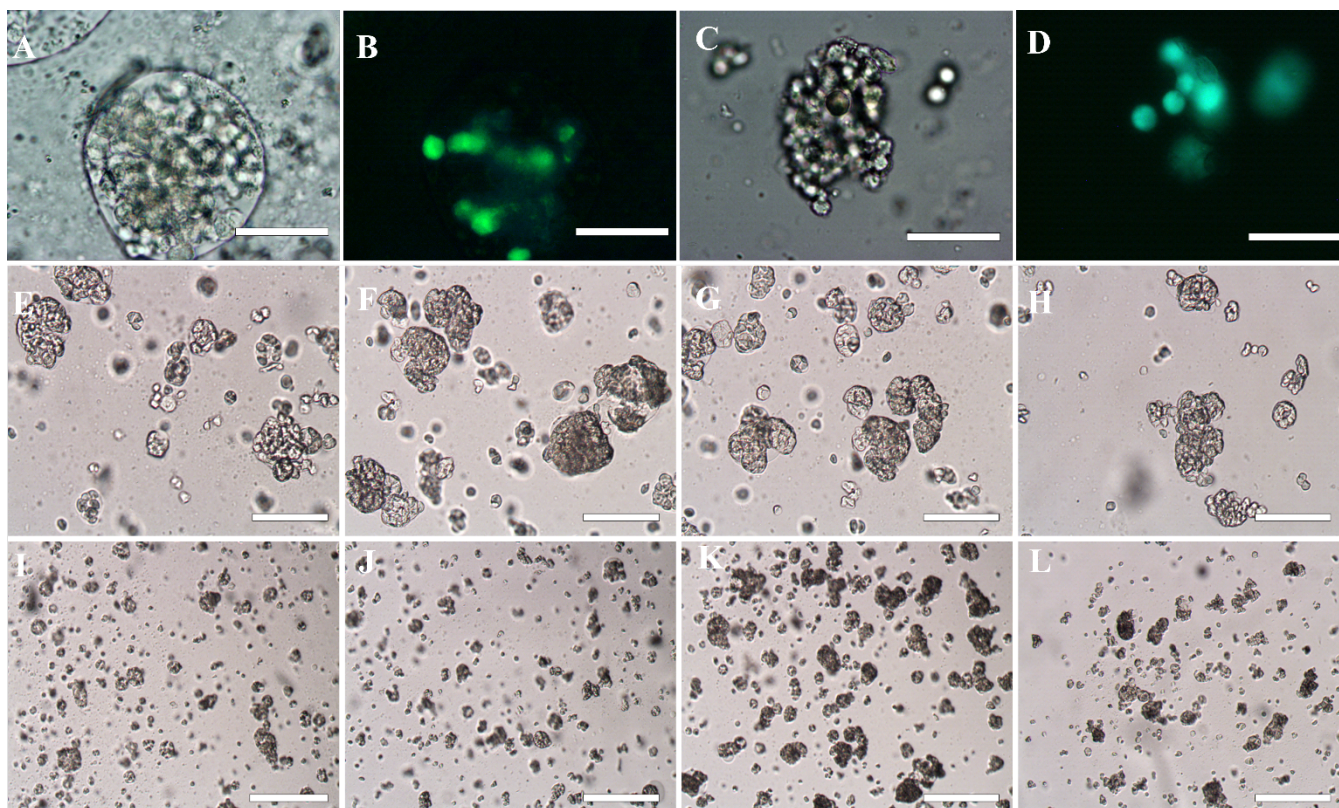


**Figure 3.** Brightfield and fluorescence microscopy images on the co-cultured clusteroids with Hep-G2:ECV304 ratio of 1:1 in the emulsion droplets (A, B) and flow state (C, D). The ECV 304 cells were solely stained to show their location within the clusteroids. Brightfield microscopy images of the collected co-culture clusteroids from the DEX/PEO w/w Pickering emulsion template with different Hep-G2/ECV cells ratio: (E, I) 1:1, (F, J) 2:1, (G, K) 5:1, (H, L) 10:1. The bar is 50  $\mu\text{m}$  for (A-D), 100  $\mu\text{m}$  for (E-H) and 200  $\mu\text{m}$  for (I-L).

### Production of ECV 304 and Hep-G2 2D monolayers and 3D co-cultured clusteroids.

The method of generating single cell type (Hep-G2 or ECV 304) clusteroids was slightly modified from the protocol introduced by Das *et al.*<sup>30</sup> The protocol is on the basis of aqueous two-phase systems, DEX/PEO solutions forming water-in-water Pickering emulsion. Briefly, the 22wt% PEO and 11 wt% Dextran solutions (DEX) were obtained by dispersing a properly weighted amount of PEO and dextran powders in deionized water. The solution needs to be magnetically stirred overnight to achieve proper solubilization. The solutions were then autoclaved (121  $^{\circ}\text{C}$ , 15 min) to obtain a sterile solution. An equal volume of the 22 wt% PEO solution 1 wt% heat-treated whey protein particle suspension (WP) was then mixed. The whey protein particles suspension was 0.45  $\mu\text{m}$  filter-sterilized prior to the mixing to avoid contamination. Then the 11 wt% PEO/WP or DEX solutions were mixed with an equal amount of DMEM/EMEM (50:50) medium supplemented with 10% FBS to obtain 5.5 wt% PEO/Medium/WP and DEX/Medium solutions. The DMEM/EMEM(50:50) medium supplemented with 10% FBS was treated as a complete medium for the co-culture

clusteroids in the following experiments. The 5.5 wt% DEX solution was utilized as the dispersed phase of the Pickering emulsion for both Hep-G2 and ECV 304 cells as both types of cells have a preferential affiliation to DEX compared to PEO phase. The cells were harvested from the T75 flasks using trypsin, and a fixed number of cells (either Hep-G2, ECV 304, or mixed cell types at different ratios) were collected and resuspended in the 50  $\mu\text{L}$  DEX/Complete medium solution. The emulsification of the w/w Pickering emulsions was achieved by gentle pumping using a syringe (BD Plastipak™ syringe) fitted with a needle (BD Microlance™ 12 needle, B.D. biosciences, Wokingham, UK). The DEX/PEO Pickering emulsions encapsulating the cells in the DEX phase were additionally compressed to allow the formation of clusteroids by adding higher condensed PEO/DMEM solution (11wt%) to reach a final PEO concentration of 8 wt%. The transportation of water from the DEX drops to the PEO phase would osmotically shrink the DEX drops further along with the encapsulated cells which forces them to adhere closer to each other. The cells were incubated in the emulsions overnight to allow the formation of cell clusteroids.

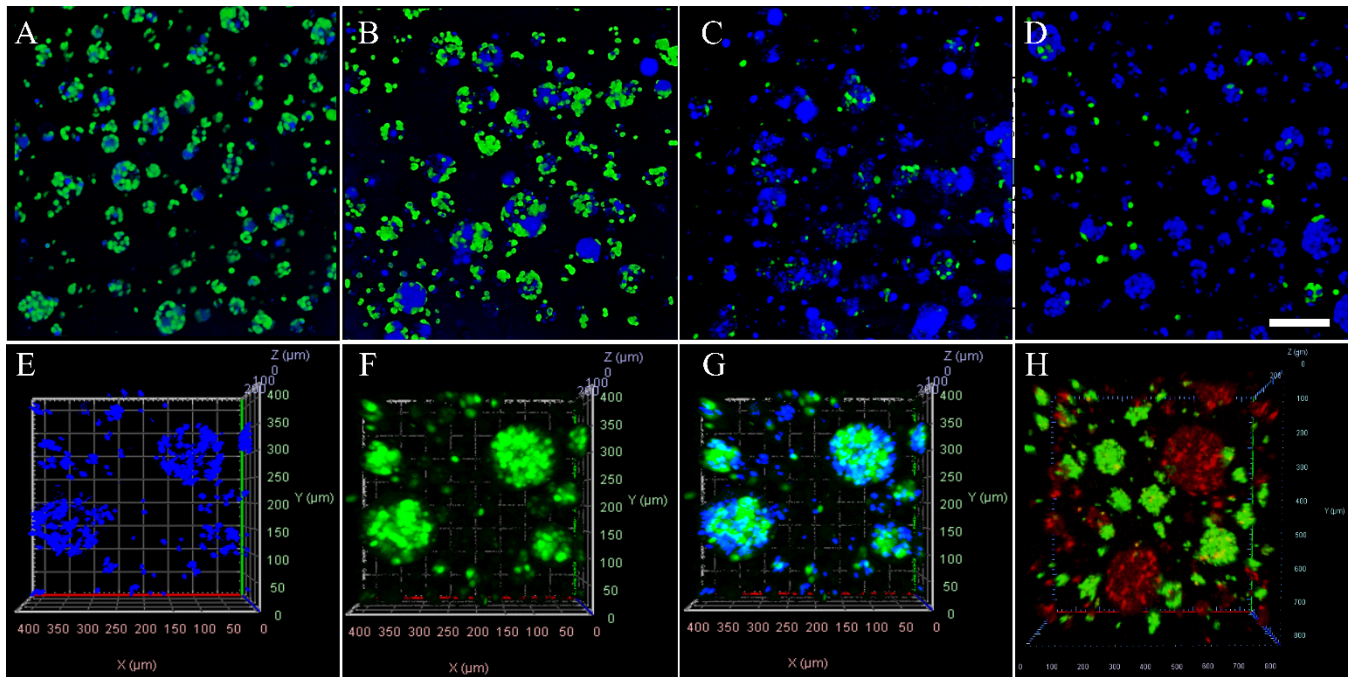


**Figure 4.** A-B: Confocal microscopy observations of co-cultured clusteroids at different Hep-G2/ECV cells ratio: (A) 1:1, (B) 2:1, (C) 5:1, (D) 10:1. (E-F) 3D Z-stacked image of E-G co-cultured Hep-G2/ECV 304 clusteroids at a cell ratio of 1:1 set at different fluorescence channels-FITC (F), DAPI (E) and Dual fluorescence (G) (H) 3D Z-stacked image of the mixture of individual Hep-G2 and ECV 304 clusteroids at a cell ratio of 1:1. In (A-D), the Hep-G2 cells and ECV 304 cells were pre-stained with DAPI and CMFDA, respectively. For distinguishing the different patterns, the Hep-G2 cells were stained with CFSE far-red, and the ECV 304 cells were stained with CFSE green in (H). The bar is 100 $\mu$ m for (A-D). The box size is 400 $\times$ 400  $\mu$ m for (E-G) and 800 $\times$ 800  $\mu$ m for (H).

Ten-fold dilution with a complete medium was used to break the w/w emulsion, after which the layer of formed clusteroids were collected with a pipette after settling at the tube bottom under gravity.

#### Long term growth of clusteroids in sodium alginate gels

The support of an ECM in the formation of endothelial networking, especially the cell sprouts in the angiogenesis process *in vitro*, is essential. Here we used sodium alginate hydrogel as an ECM to support the growth of the clusteroids. The 3 wt% sodium alginate was suspended in PBS with magnetic agitation followed by autoclaving. The 3 wt% sodium alginate gels were mixed with an equal volume of complete medium supplemented with 10% FBS to reach a final concentration of 1.5 wt% sodium alginate. After the formation of the clusteroids, the 100  $\mu$ L of the individual cell-type clusteroids or the co-culture clusteroids were seeded in 400  $\mu$ L of 1.5 wt% sodium alginate and fortified using 500  $\mu$ L of 1 wt% calcium chloride on a 24 wells plate. The culture was then incubated with 500  $\mu$ L complete media (supplemented with 10% FBS) at 37°C with 5% CO<sub>2</sub>.

#### Brightfield, fluorescence, and confocal microscopy observations

The visualization of the microstructure of the clusteroids encapsulated in the emulsion template was achieved using a fluorescence microscope (Olympus BX-51). 20  $\mu$ L samples were observed using various immersion objectives on a

concave slide under various immersion objectives. 4',6-diamidino-2-phenylindole (DAPI), or CFSE far-red were used as the fluorescent marker on the Hep-G2 cells, and CFSE green was used for the ECV 304 cells. For tracking the long-term proliferation of the co-culture clusteroids, CFSE far-red and CFSE green were used for Hep-G2 and ECV304, respectively. CFSE would permeate into cells and bind to their interior by the succinimidyl group, which would be trackable after the cell splits, generally within 14 days. The observation of the various clusteroids was also carried out using a confocal laser scanning microscope (CLSM, Zeiss LSM710). Z-stacking images were taken to generate a 3D view of the individual clusteroids and clusteroids film. The CLSM imaging was produced on precise mode.

#### Clusteroid sprouts analysis

To generate the sprouts, a low serum medium was employed. Unlike the medium introduced in the long-term culturing of the clusteroids, the complete medium was supplemented with 2 wt% FBS to stimulate the formation of sprouts. The 100  $\mu$ L of co-cultured or single-cell clusteroids were gently pipetted into 400  $\mu$ L of the 1.5wt% alginate gel before solidifying by the 500  $\mu$ L of 1wt% calcium chloride. The cultures were incubated with 500  $\mu$ L complete media supplemented with 2 wt% FBS at 37°C with 5% CO<sub>2</sub>. The clusteroids sprouts were analyzed by WimSprout assay (Wimasis image analysis, Córdoba, Spain) and the 20 longest sprouts from the clusteroids were measured on their

size to calculate the degree of angiogenesis. Objective, reproducible, and precise quantification of sprout assay images is ensured by our WimSprout online automated solution.

WimSprout is the image analysis solution to evaluate new generated sprouts during the sprouting assay. WimSprout can observe and estimate the angiogenesis process *in vitro* and identify the pro- and anti-angiogenic factors in your sprouting assay.

#### **Urea, MMP-2, and IGFBP ELISA kit**

500  $\mu$ L of the clusteroids culture's supernatant was collected at different days of culture. Urea concentration in the samples was quantified using a colorimetric endpoint assay based on acid- and heat-catalyzed condensation of urea with diacetylmonoxime (Sigma Aldrich, St Louis, USA).

The clusteroids supernatant was brought to a final volume of 50  $\mu$ L with Urea Assay Buffer and shifted to a pre-coated 96 well flasks. 50  $\mu$ L of the appropriate reaction mix was added to each of the wells. The flask was incubated for 60 min at 37 °C with horizontal shaking, protected from light during the incubation. The absorbance was measured at 570 nm (A570).

MMP-2 was quantified following the manufacturers' instructions. For the IGFBP ELISA DuoSet, 100  $\mu$ L of capture antibody was incubated in 96 well plates overnight at room temperature to allow proper coating. The capture antibody was discarded, and the 96 well plates was rinsed with 400  $\mu$ L wash buffer three times using an automatic washer. Plates were blocked by adding 300  $\mu$ L of reagent diluent to each well and incubated at room temperature for a minimum of 1 h. 100  $\mu$ L of clusteroids supernatant was added to each well and incubated for 2 h. A 100  $\mu$ L aliquot of the detection antibody, Streptavidin-HRP, and substrate solution was added in order, with a washing procedure between each step. A 50  $\mu$ L aliquot of the stop solution was added last to each well. The optical density of each well was determined immediately using a microplate reader set to 450 nm.

#### **SEM Image of the clusteroids**

The clusteroids were taken out from the sodium alginate gel using 1wt% alginate lyase, which would enzymatically degrade the gel. The clusteroids were then rinsed twice with deionized water to remove excessive sodium alginate and medium. The clusteroids were then fixed in a 1 wt% glutaraldehyde solution for 2 h at ambient temperature. The clusteroids were then left air-dried overnight before being imaged with Zeiss smart SEM software (Zeiss Evo-60 SEM, Germany).

#### **Angiogenesis array kit**

These experiments were performed according to the Human Angiogenesis Antibody Array series 1000 (Bio-technie) guidelines. To evaluate the production of angiogenesis-related genes, 1 mL of conditioned media were obtained from the co-cultured clusteroids (Hep-G2 : ECV3 04 = 1:1), Hep-G2 clusteroids, and ECV304 clusteroids embedded in the 1.5 wt% sodium alginate gel. Array membranes were incubated overnight with the 1 mL conditioned media at room temperature with gentle shaking. The medium was discarded, and

the membranes were washed with washing buffer (5 min, four times) and washing buffer II (5 min, two times), an array antibody cocktail, and a horseradish peroxidase-conjugated streptavidin antibody was incubated with the membranes for 2 h. Membranes were detected using 1X detection buffers C and D, and the array was exposed for 200 s using a chemiluminescence system (ATTO, WSE 6100 Lumi-Graph I). Blot spot intensity was calculated using GelAnalyzer 19.1 ([www.gelanalyzer.com](http://www.gelanalyzer.com)). Relative expression levels in each group were determined using the algorithm mentioned in the manufacturer's protocol.

## **Results and discussion**

### **Cell clusteroid formation in DEX-in-PEO emulsions**

3D cell culture has attracted a lot of researcher's attention in the past decades, especially in various *in vitro* drug testing. The emerging potential area of the 3D cell model is employing cell spheroids as blocks to form complex tissues. The spheroids are capable of serving as mini-organ simulations *ex vivo*, representing high gene and cytokines levels.<sup>2</sup>

Here we generated clusteroids in an aqueous two-phases system (ATPS), which contains the dextran phase, per phase, and whey protein particles. The cell clusteroids formation has been reported to have a strong relationship with the proportion of the volume fraction of DEX/PEO for several cell lines.<sup>33</sup> By changing the volume fraction and ratio of the two phases, the cells could be encapsulated and compressed into clusteroids in a short time. The overall cell concentration was first set to 10<sup>6</sup> per mL and then suspended in the 5.5 wt% DEX/Complete Medium solution before mixing with 5.5 wt% PEO/WP/Complete Medium solution at different cell ratios (Hep-G2:ECV304). After the formation of the w/w emulsion encapsulated with compressed cells, the Dextran phase would precipitate under the influence of gravity as they have a higher density than the PEO phase at any concentration (Figure S1A). In contrast, the two types of cells dispersed in complete mediums would not spontaneously form clusteroids (Figure S2). The clusteroids shrinking process was done over several hours, depending on the volume of the emulsion (Figure S1B). The DEX droplets shrinking was sufficient for the cells to form stable clusteroids, and they would accumulate at the DEX / PEO interface since their density is within 5.5 wt% Dextran and 8wt% PEO (Figure S1C).<sup>32</sup> This would avoid the direct contact of the clusteroids with the plastic surface.

To demonstrate the efficiency of the cell encapsulation, we performed preliminarily observations using a fluorescence microscope. For the observation purpose, the Hep-G2 cells and ECV304 cells were stained with DAPI (blue fluorescence) and CMFDA (green fluorescence), respectively. As shown in Figure 2, at a cell ratio of 1:1, the two types of cells coexist in multiple droplets with similar cell numbers before shrinking (Figure 2A-H). The shrinking process successfully compressed the clusteroids without influencing the cell ratio. The compressed clusteroids had structural integrity and were polydisperse in size (Figure 2E, 2I or 2H, 2L). The size of the cell clusteroids collected from the Pickering emulsion template was commonly not uniform. This

feature makes the clusteroids suitable for the tissue engineering applications instead of precise drug testing. The more concentrated PEO phase depletes the DEX droplets encapsulating the cells from water as it restores the osmotic equilibrium, and this causes them to shrink. Hence the interfacial tension of the shrinking droplets promotes the cell-

cell interactions and allows them to form more contacts. Notably, the possibility of cell co-culture in directly in the ATPS-based w/w emulsion was not mentioned in any previous reports. The results indicate the advantages of Pickering ATPS emulsion template in the high-throughput fabrication of co-cultured cell clusteroids.

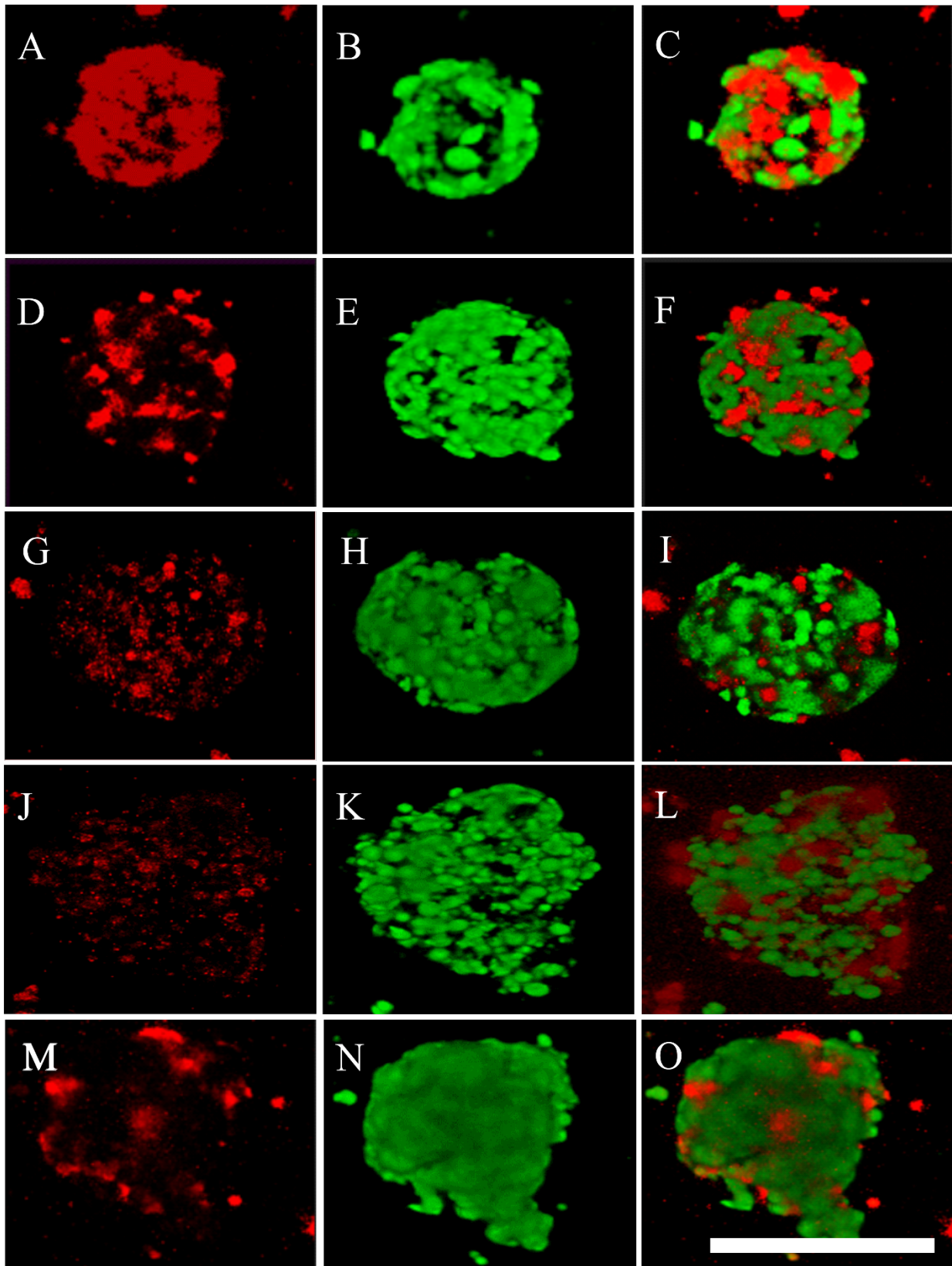


**Figure 5.** 3D Z-stacked CLSM images of co-cultured Hep-G2/ECV 304 clusteroids at a cell ratio of 1:1 after different days of culture: (A-C) day 1, (D-F) day 3, (G-I) day 5, (J-L) day 11, (M-O) day 14. The filters were set at CFSE far red (A, D, G, J, M), FITC,(B, E, H, K, N) and Dual Fluorescence (FITC/TRITC) (C, F, I, L, O) channels for imaging. The bar is 100  $\mu\text{m}$ . The Hep-G2 cells were stained with CFSE far-red, and the ECV 304 cells were stained with CFSE green.

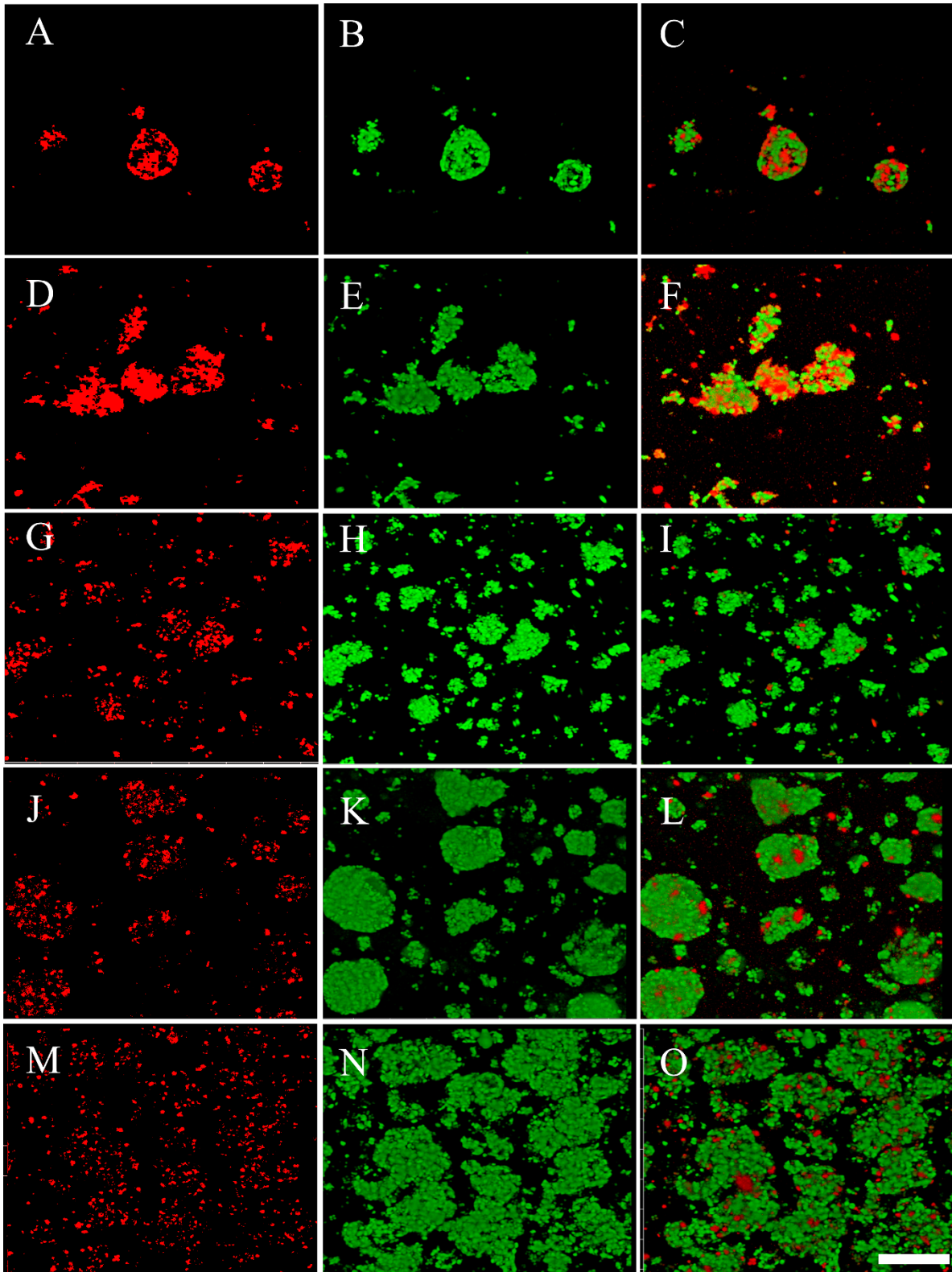


**Figure 6.** CLSM images of the proliferation of co-cultured Hep-G2/ECV 304 clusteroids at a cell ratio of 1:1 after different days of culture in 1wt% sodium alginate gel: (A-C) day 1, (D-F) day 3, (G-I) day 5, (J-L) day 11, (M-O) day 14. The filters were set at CFSE far-red/Fluorescein dual channels imaging. The bar is 100 $\mu$ m. The Hep-G2 cells were stained with CFSE far-red, and the ECV 304 cells were stained with CFSE green.

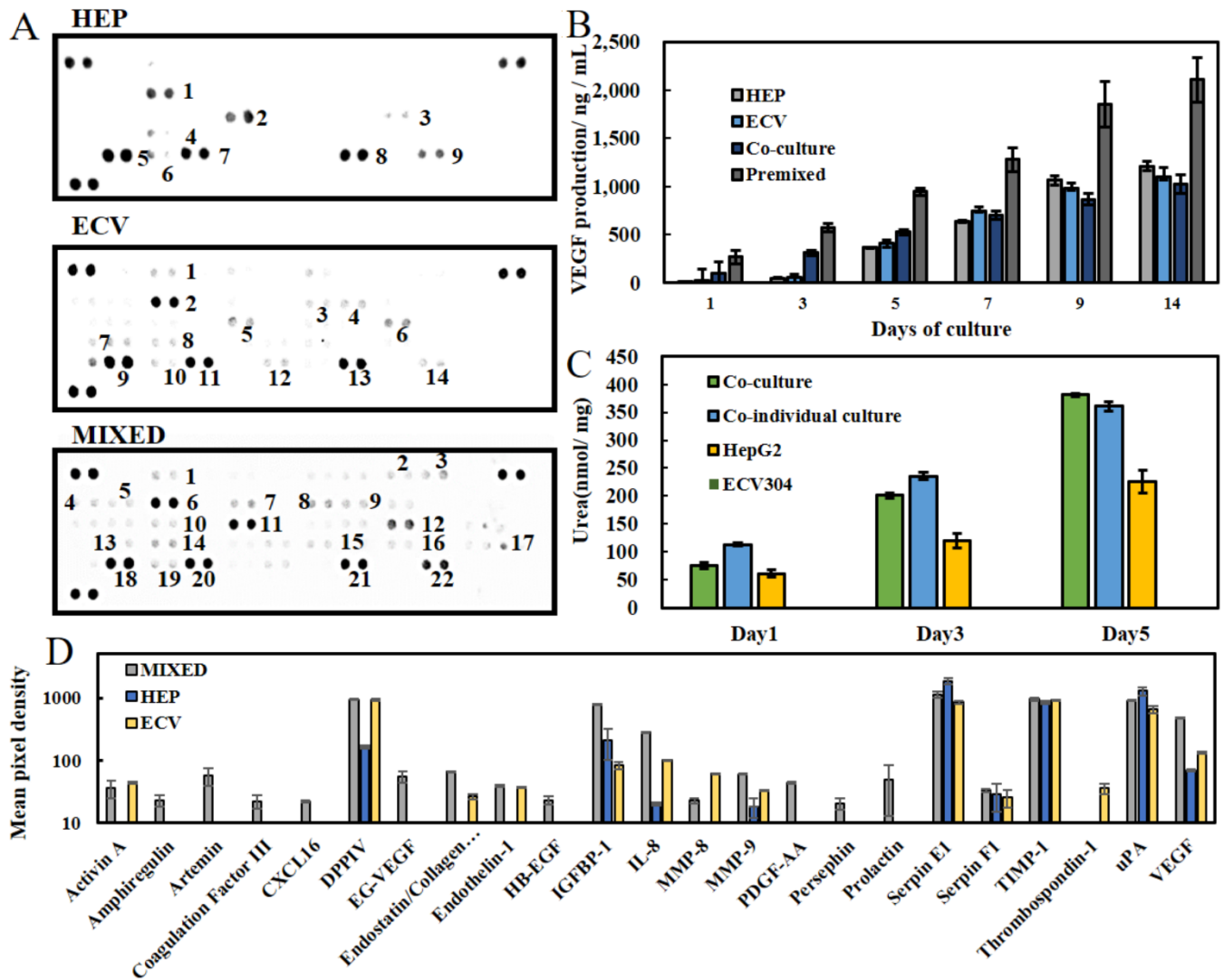


**Figure 7.** (A) Angiogenesis array membrane of individual Hep-G2 clusteroids, ECV 304 clusteroids, and the co-culture clusteroids at a cell ratio of 1:1 after 14 days of proliferation in the gel. The initial cell number were  $1 \times 10^6$  for all. (B) VEGF production of the Hep-G2 clusteroids, ECV 304 clusteroids, simple mixing of individual Hep-G2 and ECV 304 clusteroids, and the co-culture clusteroids at a cell ratio of 1:1. (C) Urea production of Hep-G2 clusteroids, ECV 304 clusteroids, and the co-culture clusteroids at a cell ratio of 1:1 after 7 days of proliferation in the gel. The initial cell number were  $1 \times 10^6$  for all. (D) Angiogenesis-related protein production in the individual Hep-G2 clusteroids, ECV 304 clusteroids, and the co-culture clusteroids at a cell ratio of 1:1 after 14 days of proliferation.

To further examine the obtained typical clusteroids compatibility in a flow state. The DEX/PEO emulsion was broken down by adding a  $10 \times$  of complete medium. The clusteroids suspension was then collected after settling and images by brightfield and fluorescence microscopy. The collected co-cultured clusteroids could maintain their structure without the further need of the emulsion template (Figure 3C, D, G, H). Certain cell segregation of the two types of cells could be easily observed. Changing the ratio of the cells slightly decreased the average diameter of the clusteroids since Hep-G2 cells have a larger size than ECV 304 (Figure 3I-L). In comparison, the individual ECV 304 cells have a slightly bigger size than the Hep-G2, about  $5 \mu\text{m}$ , which led to the formation of greater clusteroids.

Here we also observed the morphology of the individual Hep-G2 and ECV 304 clusteroids under a fluorescence microscope, and the size of the two kinds of clusteroids was measured using ImageJ. Previously, our group has reported a variety of studies on the production of different types of cell clusteroids using an ATPS Pickering emulsions template. Here we verified the feasibility of this method in mass production (Figure S3 A-J, Figure S4 A-J) of co-cultures clusteroids. The co-culture pattern of the clusteroids was further evaluated using a confocal fluorescence microscope. As can be seen in Figure 4A-D, the Hep-G2/ECV 304 proportion in the clusteroids was in correspondence to the cell ratio between the two kinds of cells suspended in the droplets.

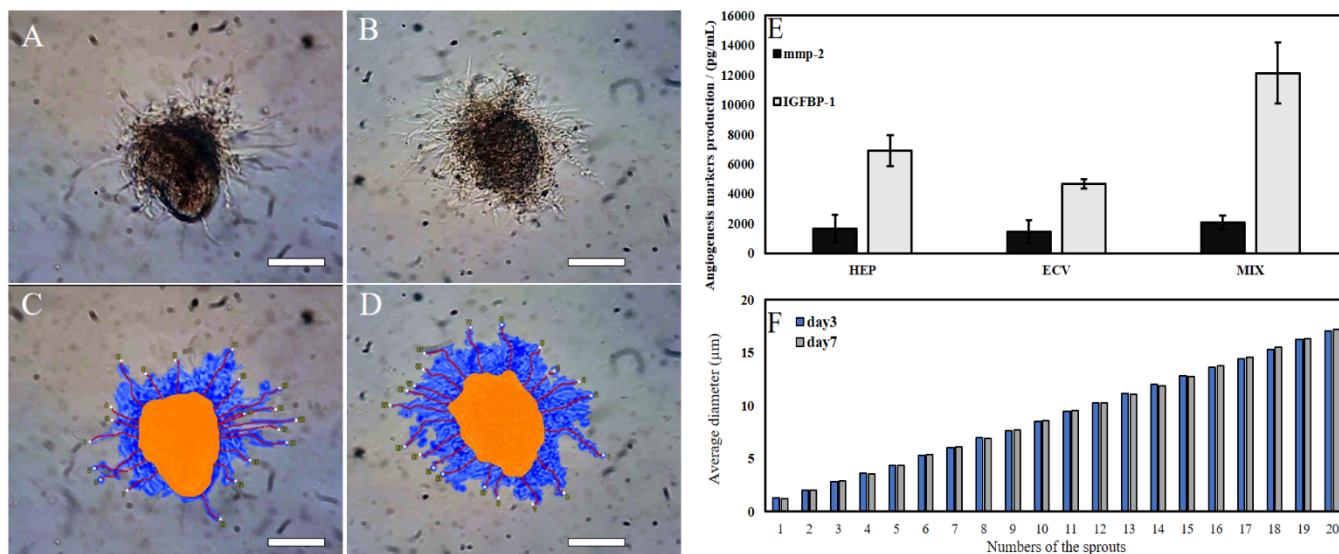


**Figure 8.** Bright field observation (A, B) and the corresponding Wimasprouts analysis (C, D) of the co-culture clusteroids at a cell ratio of 1:2 (Hep-G2 : ECV 304) after 3 days of culture in 1wt% sodium alginate gel. (E) MMP-2 and IGFBP-1 production of the individual Hep-G2 clusteroids, ECV 304 clusteroids, and the co-culture clusteroids at a cell ratio of 1:1 after 14 days of proliferation in the gel (The initial cell number were  $1 \times 10^6$  for all). (F) The length of the sprouts in (C, D). The bar is 50  $\mu\text{m}$ .

The size of the co-cultured clusteroids showed a decremental trend with increased Hep-G2 proportion, from 68  $\mu\text{m}$  to 45  $\mu\text{m}$ . Relative to the result in Figure S3, S4, which indicates that the ECV 304 has a bigger size in individual or clustered cell form. The 3D Z-stacked images of the co-cultured Hep-G2/ECV 304 clusteroids at a cell ratio of 1:1 set at different fluorescence channels were shown in Figure 4E-G, as could be clearly seen that the two kinds of cells self-organized into integral clusteroids. Figure 4H shows the 3D Z-stacked image of the mixture of individual Hep-G2 and ECV 304 clusteroids at a cell ratio of 1:1, which was set as a control to check if the mixture of two types of individual cell clusteroids did not migrate into each other to form co-cultured clusteroids. Taken together, by altering the initial cell proportion, co-cultured clusteroids with different cell ratios could be obtained using the w/w emulsion template.

#### Long term proliferation of the co-cultured cell clusteroids in sodium alginate gel

Tissue engineering and drug testing purposes are commonly discussed in the application of vascularized cell clusters.<sup>34,35</sup> The number of cell clusters required for these two purposes is of distinct differences. To meet these two downstream applications, we placed different amounts of cell clusteroids in the gel.

A fixed amount of co-cultured clusteroids ( $1 \times 10^6$  cells per mL for layered cell formation and  $1 \times 10^5$  per mL for single cell type clusteroid observation) was moved to 24-well microplates before mixing with the sodium alginate solution. This clusteroid-hydrogel composite was solidified using calcium chloride solution, which allows the long-term proliferation of clusteroids in a supporting matrix. The proliferation of the clusteroids, which were labeled by generational dyes (CFSE green for Hep-G2 and CFSE far-red for ECV 304), was continually monitored by fluorescence microscopy over a

period of 14 days. The results, as shown in Figure 5 the single clusteroid with Hep-G2: ECV 304 ratio of 1:1 indicate that the clusteroids would proliferate slowly into a bigger size. The green signal, which tracks ECV 304 cells, dominated the co-cultured clusteroids after day 5 as they have a significantly faster doubling time than the Hep-G2 cells. In the 2D monolayer culture, the ECV 304 could be split 1 to 16 in one passage (Figure 5). With an increased Hep-G2 cell ratio (Hep-G2: ECV 304=5:1), the two types of cells generally were of similar quantity after 14 days of proliferation (Figure S4). For the production of the clusteroids layer, a higher cell concentration ( $1 \times 10^6$  per mL) was used to facilitate the contact between clusteroids, which would faster lead to clusteroids fusion (Figure S10). The clusteroids proliferate to a greater size before appropriate clusteroids interfaces were reached. Similarly, in the proliferation of the larger amount of cell clusteroids at Hep-G2 : ECV 304 ratio of 1:1, the domination of the ECV304 is also obvious. The individual clusteroids firstly grew until the space between them was occupied, then the clusteroids started fusing into a tissue-like 3D compacted layer. The confocal microscopy tracking of the 3D layered formation of clusteroids indicates the same layout. The thickness and dark color of the sodium alginate gel might make the light difficult to passing through, resulting in lower resolution figures collected from the 3D confocal images. The proliferation of the ECV304 cells was much faster and the green fluorescence signal of their CFSE stain was dominant on the clusteroids at the end of the period of observation (Figure 6). Overall, these results indicate that the w/w APTS Pickering emulsion template would be an excellent platform for the fast preparation of either individual or numerous co-cultured Hep-G2/ECV 304 at the different ratios for drug testing or as a model for tissue engineering applications. In order to verify

that our co-culture method enhances the cell-to-cell contact, a series of cell functionality test were carried out.

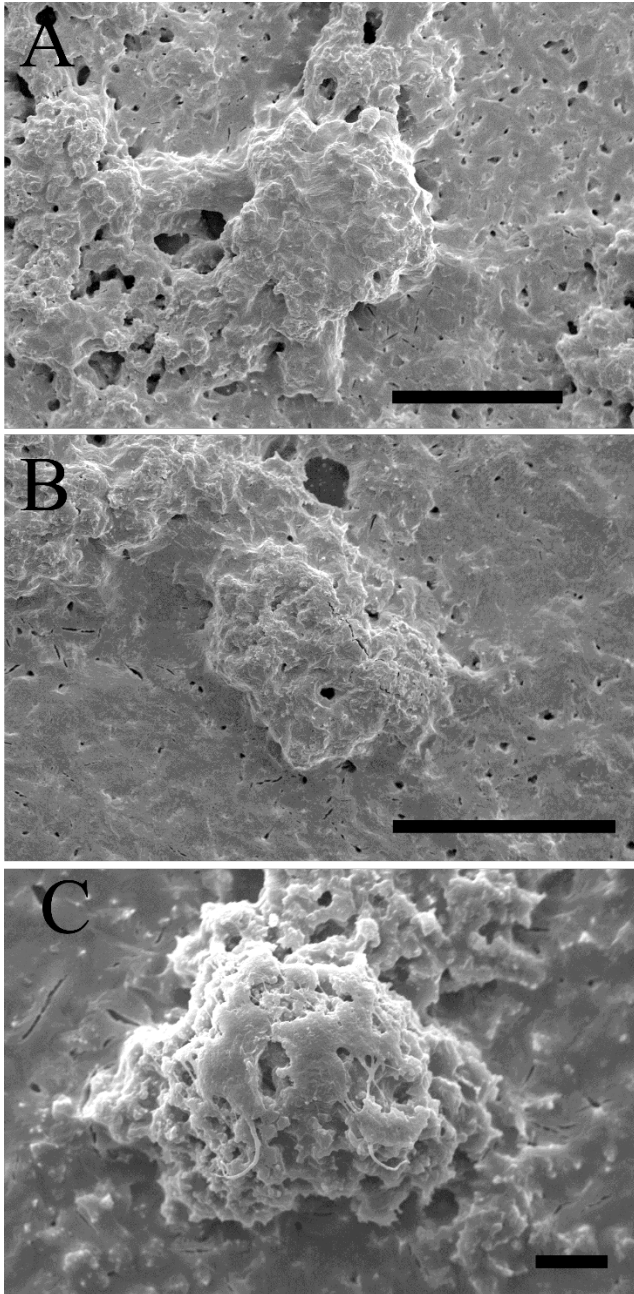


**Figure 9.** SEM observation of the (A) single cell type Hep-G2 clusteroids, (B) single cell type ECV 304 clusteroids, (C) Co-culture of Hep-G2 : ECV 304 clusteroids at a ratio of 1:1.

#### Angiogenic factors produced by co-cultured clusteroids

The main purpose of employing ECV 304 and Hep-G2 cells co-culturing is to identify the feasibility of vascularization of the clusteroids in a co-culture pattern. We primarily collected the supernatant serum of the clusteroids cultures to carry out a cocktail antibody angiogenesis assay. The co-cultured clusteroids were compared to individual ECV 304 and

Hep-G2 clusteroids on the production of various angiogenesis-related genes. As can be seen from Figure 7A, the production of a wide range of angiogenesis-related genes was boosted, and several genes were triggered in the co-culture pattern. The detailed detected genes in the three different types of clusteroids are shown in Figure S7. The feature of these genes on whether they are pro-angiogenesis or anti-angiogenesis is given in Figure S8.

It could be clearly observed that the co-cultures showed a dramatic increase in the expression of IGFBP-1, IL-8, and VEGF when compared to ECV 304 and HEP-G2 single cell type clusteroids (Figure 7D). The production of seven genes was only detected in the co-cultured clusteroids, such as Activin A, Amphiregulin, Artemin, and HB-EGF, which are all believed to be pro-angiogenic (Figure S7). The production level of TIMP-1, Serpin-F1, and Serpin-E1 was not enhanced. Serpin-E1 is considered as an inhibitor of tissue plasminogen activator (tPA) and urokinase (uPA).<sup>36</sup> Serine proteases (Serpin E1, Serpin F1) are specifically recognized, negative angiogenic regulators.<sup>37</sup> The encoded protein is secreted and strongly inhibits angiogenesis. The TIMP production was also highly connected to the inhibition of angiogenesis by serving as natural inhibitors of the matrix metalloproteinases (MMPs).<sup>38</sup> In conclusion, the angiogenesis array showed that the co-cultured platform triggered the release of seven pro-angiogenesis-related proteins, which were not found in either ECV304 or HEP-G2 clusteroids. The production of the three anti-angiogenesis proteins, TIMP, Serpin-F1, and serpin-E1, was not enhanced. The imbalance of anti- and pro-angiogenic proteins could also strongly indicate the efficiency of co-culturing patterns in triggering the blood vessel formation.

In order to verify the accuracy of the angiogenesis kit, we have performed several ELISA kits included VEGF, IGFBP-1, MMP-2, and also a urea assay. VEGF production is one the most commonly discussed angiogenesis-related cytokines as it is used as a stimulator on *in vitro* spheroid vascularization.<sup>39,40</sup> We have tested the VEGF production in four patterns of clusteroids culture over 14 days of culture. It could be seen from Figure 7B that the overall production of the co-cultured pattern was two times higher than the rest three patterns. This is also consistent with the result in Figure 7D. Another major compound-related Hep-G2 functionality is the urea production, which also serves an important role in the metabolism of nitrogen-containing compounds by animals and is the main nitrogen-containing substance in the urine of mammals. The production of urea was low on day 1, which might be attributed to the adaptation stage in the early stage of cell co-culture (Figure 7C). However, the production on day 3 has surpassed the other patterns by a huge margin.

#### Sprouting in cell clusteroids

The cell spheroid-based sprouting assay is a well-established and robust method to study the influence of genetic alterations or pharmacological compounds on capillary-like tube formation of primary cultured endothelial cells. The most commonly used ECM is Matrigel. Here we employed sodium alginate hydrogel to perform the cell sprouting assay.

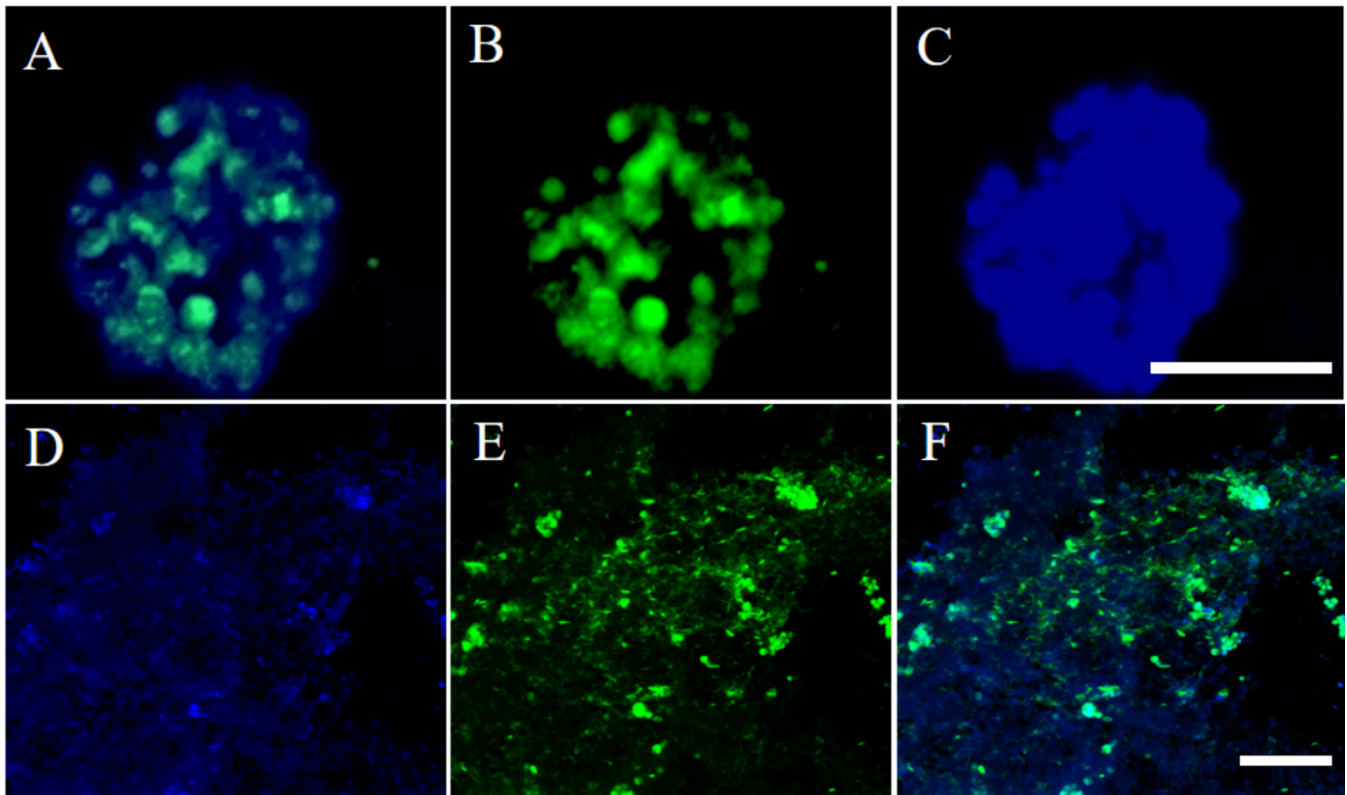


**Figure 10.** Confocal observation of the Co-culture of Hep-G2 clusteroids and ECV 304 clusteroids at a ratio of 1:1 with CD34-FITC conjugated labeling on individual clusteroid (A-C) and (D-F) formed layer of clusteroids. The bar is 200  $\mu\text{m}$  for (D-F).

The length of the clusteroids' sprouts could be used to describe the extent of angiogenesis. In our tests, we have observed that at the Hep-G2 : ECV 304 ratio of 1:2, the clusteroids may form long sprouts into the sodium alginate hydrogel (Figure 8A-D). The distinct cell ratio needed for sprouts formation might be attributed to the unique cell-cell interaction. The single cell type, Hep-G2 or ECV304, cell clusteroids were not capable of forming such capillary structures. When performing the 3D endothelial cell sprouts assay, many authors add VEGF externally to stimulate the out-spread of sprouts. However, in the co-culture clusteroids Hep-G2 and ECV 304 cells we observed generation of sprouts without the addition of any exogenous substances. The Hep-G2 would work as a VEGF drive engine to irritate the ECV 304 cells to sprout.<sup>41</sup> However, after the clusteroids sprouted to about 10  $\mu\text{m}$  on day 3, clusteroids would only generate more sprouts instead of keep stretching the existed ones (Figure 8F).

The MMP-2 is a protein of the matrix metalloproteinase (MMP) family that is involved in the breakdown of ECM in normal physiological processes, such as embryonic development, reproduction, and tissue remodeling as well as in disease processes, such as arthritis and metastasis.<sup>42</sup> MMP-2 is a crucial protein when the clusteroids sprouts into the ECM.<sup>43</sup> The production of MMP-2 in the co-cultured clusteroids was slightly enhanced, about two times higher than the individual ECV 304 or Hep-G2 clusteroids after 14 days of

culture (Figure 8E). This might be either attributed to the fact that the sprouts stopped growing longer after 3 days of culture. Previously reported in culturing carcinoma cells/E.C.s, spheroids observed similar results that without the addition of VEGF, the carcinoma cells would stimulate co-cultured spheroids to sprouts.<sup>44,45</sup> However, the sprouting ability of the E.C.s would be reduced in the co-culture pattern.<sup>44</sup> SEM imaging of our clusteroid samples also indicated the existence of several tails-like structures in the co-cultured clusteroids (Figure 9C), which was not detected in the individual clusteroids (Figure 9A, B).

#### Immunohistochemistry

Immunohistochemistry (IHC) is the most common application of immunostaining. It involves the process of selectively identifying antigens (proteins) in cells of a tissue section by exploiting the principle of antibodies binding specifically to antigens in biological tissues. ECV 304 cells cultured on collagen I are strongly positive for CD34 (Blintegrin), weakly-positive for CD31, and negative for von Willebrand factor.<sup>46</sup> So here, the endothelial phenotype of co-cultured clusteroids was evaluated by immunofluorescent staining for CD34 of endothelial cell surface markers. CD34 is the marker to select for endothelial cells with a tip cell phenotype *in vitro*. CD34 is a highly glycosylated transmembrane cell surface glycoprotein, expressed by hematopoietic stem and progenitor and on the luminal cell membrane of

quiescent endothelial cells of small blood vessels and lymphatics.<sup>47</sup> CD 34 was detected in a single co-cultured clusteroids and the co-cultured clusteroids layer (Figure 10). The CD34 staining clearly indicated the tubule network in the co-cultured clusteroids and would be a shred of additional evidence to support the formation of the blood vessels within the co-cultured clusteroids. To study the angiogenic behaviours of cancer cells *in vivo* in detail, primary cell line or biopsy tissue might be used for precise cellular response between the carcinoma and endothelial cells. Adherent junction proteins like VE-cadherin, cytoskeleton proteins were key factors that would be tested in these co-culture models in future studies.

## Conclusions

Here we developed a facile and high throughput method to produce 3D co-culture of mixed cell Hep-G2/ECV304 clusteroids. The co-cultured clusteroids with different cell ratios could be obtained in the w/w Aqueous Two-Phase Pickering emulsion droplets stabilized by whey protein particles. The long-term tracking of the co-cultured clusteroids was successfully carried out using a fluorescence and confocal microscopy. The proliferation pattern of the single cell type and large amounts of the co-cultured clusteroids was characterized. By changing the ratio to 1:2 (Hep-G2 : ECV 304) of the two cell types and applying a low serum medium, the co-cultured clusteroids could sprout into the ECM formed by sodium alginate hydrogel. Various angiogenesis genes production was found to be significantly enhanced in the co-cultured clusteroid pattern. Enhanced production of VEGF, urea, and IGFBP also indicated the angiogenesis progress triggered by the co-culture pattern. Immunohistochemistry assay also suggested the presence of the angiogenesis-related marker CD34. This co-culturing platform provides researchers with a robust approach for fabrication of various co-cultured, and potentially even tri-cultured clusteroids with the required cell functionality. The cells utilized in our experiments could be swapped with any cell lines or primary cells cultures. This work would fill in the absence of an easy-to-handle, high throughput production of vascularized co-cultured 3D clusteroids *in vitro*, which are expected to be utilized in drug testing and a variety of tissue engineering applications.

## ASSOCIATED CONTENT

### Supporting Information

The Supporting Information is available free of charge on the ACS Publications website at DOI: 10.1021/

- (i) Clusteroids formation in the w/w Pickering emulsion template; (ii) Observation of the co-culture cells in complete medium; (iii) Observation of the HepG2 clusteroids in different forms; (iv) Average diameter of the various forms of ECV304 and Hep-G2 cells; (v) Observation of the ECV304 clusteroids in different forms; (vi) Average diameter of the co-cultured clusteroids at different cell ratio; (vii) Bright field observation of the single Hep-G2 and ECV304 in sodium alginate gel without sprouts;

- (viii) Bright field observation and the corresponding Wimasprouts analysis of the co-culture clusteroids at a cell ratio of 1:2 (Hep-G2:ECV 304) after 3 days of culture in sodium alginate gel; (ix) The effect of the Angiogenesis-related genes on the vascularization process; (x) Angiogenesis-related protein production in the individual Hep-G2 clusteroids, ECV 304 clusteroids, and the co-culture clusteroids at a cell ratio of 1:1 after 14 days of proliferation; (xi) CLSM images of the proliferation of co-cultured Hep-G2/ECV 304 clusteroids at a cell ratio of 5:1 after different days of culture in 1wt% sodium alginate gel; (xii) Observation of the co-culture growth in sodium alginate gel at different days of culture (PDF).

## AUTHOR INFORMATION

\*Corresponding Author

Email: [vesselin.paunov@nu.edu.kz](mailto:vesselin.paunov@nu.edu.kz)

### ORCID

Anheng Wang: 0000-0001-6616-2828  
Leigh Madden: 0000-0002-1503-1147  
Vesselin N. Paunov: 0000-0001-6878-1681

## Funding Sources

Chinese Scholarship Council for the financial support of A.W. Ph.D. studies (CSC NO.201908210332).

## Notes

The authors declare no competing financial interest.

## Author Contributions

The manuscript was written through contributions of all authors. A.W. performed the experiments, prepared the graphs and the first draft of the manuscript. V.N.P. provided the project idea, directed the project, supervised the work of A.W. and edited the manuscript. L.A.M. co-supervised A.W., provided training, technical guidance and edited the manuscript. All authors have given approval to the final version of the manuscript.

## ACKNOWLEDGMENTS

A. W. thanks the Chinese Scholarship Council for the financial support of his Ph.D. studies (CSC NO.201908210332). The authors would like to thank the SEM technician Mr. Timothy Dunstan (University of Hull), for his assistance during this project.

## ABBREVIATIONS

EPS, extracellular polymeric substance; MHB, Mueller Hilton Broth; MHA, Mueller Hilton agar; CFU, colony forming unit; SEM, Scanning electron microscope; TEM, Transmission electron microscope; AFM, Atomic force microscope.

## REFERENCES

- (1) Wang, A.; Madden, L. A.; Paunov, V. N. Advanced Biomedical Applications Based on Emerging 3D Cell Culturing Platforms. *J. Mater. Chem. B Mater. Biol. Med.* **2020**, *8* (46), 10487–10501. DOI:10.1039/D0TB01658F F
- (2) Ravi, M.; Paramesh, V.; Kaviya, S. R.; Anuradha, E.; Solomon, F. D. P. 3D Cell Culture Systems: Advantages and Applications:

- 3D Cell Culture Systems. *J. Cell. Physiol.* **2015**, 230 (1), 16–26. DOI: 10.1002/jcp.24683
- (3) Jensen, C.; Teng, Y. Is It Time to Start Transitioning from 2D to 3D Cell Culture? *Front. Mol. Biosci.* **2020**, 7, 33. DOI: 10.3389/fmolb.2020.00033
- (4) Fontoura, J. C.; Viezzer, C.; Dos Santos, F. G.; Ligabue, R. A.; Weinlich, R.; Puga, R. D.; Antonow, D.; Severino, P.; Bonorino, C. Comparison of 2D and 3D Cell Culture Models for Cell Growth, Gene Expression and Drug Resistance. *Mater. Sci. Eng. C Mater. Biol. Appl.* **2020**, 107 (110264), 110264. DOI: 10.1016/j.msec.2019.110264.
- (5) Andersen, M. L.; Winter, L. M. F. Animal Models in Biological and Biomedical Research - Experimental and Ethical Concerns. *An. Acad. Bras. Cienc.* **2019**, 91 (suppl 1), e20170238. DOI:10.1590/0001-3765201720170238. Epub 2017 Sep 4.
- (6) Varga, O. E.; Hansen, A. K.; Sandøe, P.; Olsson, I. A. S. Validating Animal Models for Preclinical Research: A Scientific and Ethical Discussion. *Altern. Lab. Anim.* **2010**, 38 (3), 245–248. DOI: 10.1177/026119291003800309
- (7) Gilazieva, Z.; Ponomarev, A.; Rutland, C.; Rizvanov, A.; Solovyeva, V. Promising Applications of Tumor Spheroids and Organoids for Personalized Medicine. *Cancers (Basel)* **2020**, 12 (10), 2727. DOI: 10.3390/cancers12102727
- (8) Guillaume, L.; Rigal, L.; Fehrenbach, J.; Severac, C.; Ducommun, B.; Lobjois, V. Characterization of the Physical Properties of Tumor-Derived Spheroids Reveals Critical Insights for Pre-Clinical Studies. *Sci. Rep.* **2019**, 9 (1), 6597. DOI:10.1038/s41598-019-43090-0
- (9) Hirschhaeuser, F.; Menne, H.; Dittfeld, C.; West, J.; Mueller-Klieser, W.; Kunz-Schughart, L. A. Multicellular Tumor Spheroids: An Underestimated Tool Is Catching up Again. *J. Biotechnol.* **2010**, 148 (1), 3–15. DOI: 10.1016/j.jbiotec.2010.01.012.
- (10) Mironov, V.; Visconti, R. P.; Kasyanov, V.; Forgacs, G.; Drake, C. J.; Markwald, R. R. Organ Printing: Tissue Spheroids as Building Blocks. *Biomaterials* **2009**, 30 (12), 2164–2174. DOI: 10.1016/j.biomaterials.2008.12.084
- (11) Mattix, B.; Olsen, T. R.; Gu, Y.; Casco, M.; Herbst, A.; Simionescu, D. T.; Visconti, R. P.; Kornev, K. G.; Alexis, F. Biological Magnetic Cellular Spheroids as Building Blocks for Tissue Engineering. *Acta Biomater.* **2014**, 10 (2), 623–629. DOI:10.1016/j.actbio.2013.10.021. Epub 2013 Oct 28.
- (12) Kim, E. M.; Lee, Y. B.; Kim, S.-J.; Park, J.; Lee, J.; Kim, S. W.; Park, H.; Shin, H. Fabrication of Core-Shell Spheroids as Building Blocks for Engineering 3D Complex Vascularized Tissue. *Acta Biomater.* **2019**, 100, 158–172. DOI: 10.1016/j.actbio.2019.09.028. Epub 2019 Sep 19
- (13) Mukomoto, R.; Nashimoto, Y.; Terai, T.; Imaizumi, T.; Hiramoto, K.; Ino, K.; Yokokawa, R.; Miura, T.; Shiku, H. Oxygen Consumption Rate of Tumour Spheroids during Necrotic-like Core Formation. *Analyst* **2020**, 145 (19), 6342–6348. DOI:10.1039/D0AN00979B
- (14) Folkman, J.; Haudenschild, C. Angiogenesis in Vitro. *Nature* **1980**, 288 (5791), 551–556. DOI:10.1038/288551a0.
- (15) Carmeliet, P. VEGF as a Key Mediator of Angiogenesis in Cancer. *Oncology* **2005**, 69 Suppl 3 (3), 4–10. DOI:10.1159/000088478. Epub 2005 Nov 21.
- (16) Benedito, R.; Roca, C.; Sörensen, I.; Adams, S.; Gossler, A.; Frutiger, M.; Adams, R. H. The Notch Ligands Dll4 and Jagged1 Have Opposing Effects on Angiogenesis. *Cell* **2009**, 137 (6), 1124–1135. DOI:10.1016/j.cell.2009.03.025.
- (17) Karagiannis, E. D.; Popel, A. S. Distinct Modes of Collagen Type I Proteolysis by Matrix Metalloproteinase (MMP) 2 and Membrane Type I MMP during the Migration of a Tip Endothelial Cell: Insights from a Computational Model. *J. Theor. Biol.* **2006**, 238 (1), 124–145. DOI: 10.1016/j.jtbi.2005.05.020. Epub 2005 Jul 6.
- (18) Yana, I.; Sagara, H.; Takaki, S.; Takatsu, K.; Nakamura, K.; Nakao, K.; Katsuki, M.; Taniguchi, S.-I.; Aoki, T.; Sato, H.; Weiss, S. J.; Seiki, M. Crosstalk between Neovessels and Mural Cells Directs the Site-Specific Expression of MT1-MMP to Endothelial Tip Cells. *J. Cell Sci.* **2007**, 120 (Pt 9), 1607–1614. DOI: 10.1242/jcs.000679. Epub 2007 Apr 3.
- (19) Vandekerke, S.; Dewerchin, M.; Carmeliet, P. Angiogenesis Revisited: An Overlooked Role of Endothelial Cell Metabolism in Vessel Sprouting. *Microcirculation* **2015**, 22 (7), 509–517. DOI: 10.1111/micc.12229.
- (20) Shamloo, A.; Heilshorn, S. C. Matrix Density Mediates Polarization and Lumen Formation of Endothelial Sprouts in VEGF Gradients. *Lab Chip* **2010**, 10 (22), 3061–3068. DOI:10.1039/C005069E
- (21) Twardowski, R. L.; Black, L. D., III. Cardiac Fibroblasts Support Endothelial Cell Proliferation and Sprout Formation but Not the Development of Multicellular Sprouts in a Fibrin Gel Co-Culture Model. *Ann. Biomed. Eng.* **2014**, 42 (5), 1074–1084. DOI:10.1007/s10439-014-0971-2. Epub 2014 Jan 17.
- (22) Wirz, W.; Antoine, M.; Tag, C. G.; Gressner, A. M.; Korff, T.; Hellerbrand, C.; Kiefer, P. Hepatic Stellate Cells Display a Functional Vascular Smooth Muscle Cell Phenotype in a Three-Dimensional Co-Culture Model with Endothelial Cells. *Differentiation* **2008**, 76 (7), 784–794. DOI: 10.1111/j.1432-0436.2007.00260.x. Epub 2008 Jan 3.
- (23) Pfisterer, L.; Korff, T. Spheroid-Based in Vitro Angiogenesis Model. In *Methods in Molecular Biology*; Springer New York: New York, NY, 2016; pp 167–177. DOI: 10.1007/978-1-4939-3628-1\_11.
- (24) Timmins, N.; Dietmair, S.; Nielsen, L. Hanging-Drop Multicellular Spheroids as a Model of Tumour Angiogenesis. *Angiogenesis* **2004**, 7 (2), 97–103. DOI: 10.1007/s10456-004-8911-7.
- (25) Shah, S.; Lee, H.; Park, Y. H.; Jeon, E.; Chung, H. K.; Lee, E. S.; Shim, J. H.; Kang, K.-T. Three-Dimensional Angiogenesis Assay System Using Co-Culture Spheroids Formed by Endothelial Colony Forming Cells and Mesenchymal Stem Cells. *J. Vis. Exp.* **2019**, No. 151, e60032. DOI: 10.3791/60032.
- (26) Correa de Sampaio, P.; Auslaender, D.; Krubasik, D.; Failla, A. V.; Skepper, J. N.; Murphy, G.; English, W. R. A Heterogeneous in Vitro Three Dimensional Model of Tumour-Stroma Interactions Regulating Sprouting Angiogenesis. *PLoS One* **2012**, 7 (2), e30753. DOI:10.1371/journal.pone.0030753
- (27) Nashimoto, Y.; Okada, R.; Hanada, S.; Arima, Y.; Nishiyama, K.; Miura, T.; Yokokawa, R. Vascularized Cancer on a Chip: The Effect of Perfusion on Growth and Drug Delivery of Tumor Spheroid. *Biomaterials* **2020**, 229 (119547), 119547. DOI: 10.1016/j.biomaterials.2019.119547. Epub 2019 Oct 17.
- (28) Atefi, E.; Lemmo, S.; Fyffe, D.; Luker, G. D.; Tavana, H. High Throughput, Polymeric Aqueous Two-Phase Printing of Tumor Spheroids. *Adv. Funct. Mater.* **2014**, 24 (41), 6509–6515. DOI: 10.1002/adfm.201401302.
- (29) Lemmo, S.; Atefi, E.; Luker, G. D.; Tavana, H. Optimization of Aqueous Biphasic Tumor Spheroid Microtechnology for Anti-Cancer Drug Testing in 3D Culture. *Cell. Mol. Bioeng.* **2014**, 7 (3), 344–354. DOI: 10.1007/s12195-014-0349-4.
- (30) Das, A. A. K.; Filby, B. W.; Geddes, D. A.; Legrande, D.; Paunov, V. N. High Throughput Fabrication of Cell Spheroids by Templating Water-in-Water Pickering Emulsions. *Mater. Horiz.* **2017**, 4 (6), 1196–1200. DOI:10.1039/C7MH00677B
- (31) Wang, A.; Weldrick, P. J.; Madden, L. A.; Paunov, V. N. Biofilm-Infected Human Clusteroid Three-Dimensional Coculture Platform to Replace Animal Models in Testing Antimicrobial Nanotechnologies. *ACS Appl. Mater. Interf.* **2021**, 13 (19), 22182–22194. DOI:10.1021/acsami.1c02679
- (32) Wang, A.; Weldrick, P. J.; Madden, L. A.; Paunov, V. N. Enhanced Clearing of Candida Biofilms on a 3D Urothelial Cell in Vitro

- Model Using Lysozyme-Functionalized Fluconazole-Loaded Shellac Nanoparticles. *Biomater. Sci.* 2021, 9 (20), 6927–6939. DOI:10.1039/D1BM01035B
- (33) Xiong, W.-C.; Simon, S. ECV304 Cells: An Endothelial or Epithelial Model? *J. Biol. Chem.* 2011, 286 (41), 1e21. DOI: 10.1074/jbc.N111.261073
- (34) Kim, S.; Kim, E. M.; Yamamoto, M.; Park, H.; Shin, H. Engineering Multi-cellular Spheroids for Tissue Engineering and Regenerative Medicine. *Adv. Healthc. Mater.* 2020, 9 (23), 2000608. DOI:10.1002/adhm.202000608
- (35) Laschke, M. W.; Menger, M. D. Spheroids as Vascularization Units: From Angiogenesis Research to Tissue Engineering Applications. *Biotechnol. Adv.* 2017, 35 (6), 782–791. DOI: 10.1016/j.biotechadv.2017.07.002.
- (36) Fortenberry, Y. M. Plasminogen Activator Inhibitor-1 Inhibitors: A Patent Review (2006 – Present). *Expert Opin. Ther. Pat.* 2013, 23 (7), 801–815. DOI: 10.1517/13543776.2013.782393.
- (37) Ratushnyy, A.; Ezdakova, M.; Yakubets, D.; Buravkova, L. Angiogenic Activity of Human Adipose-Derived Mesenchymal Stem Cells under Simulated Microgravity. *Stem Cells Dev.* 2018, 27 (12), 831–837. DOI:10.1089/scd.2017.0262. Epub 2018 Mar 12.
- (38) Ito, A.; Sato, T.; Iga, T.; Mori, Y. Tumor Necrosis Factor Bifunctionally Regulates Matrix Metalloproteinases and Tissue Inhibitor of Metalloproteinases (TIMP) Production by Human Fibroblasts. *FEBS Lett.* 1990, 269 (1), 93–95. DOI: 10.1016/0014-5793(90)81127-a.
- (39) Pepper, M. S.; Mandriota, S. J.; Jeltsch, M.; Kumar, V.; Alitalo, K. Vascular Endothelial Growth Factor (VEGF)-C Synergizes with Basic Fibroblast Growth Factor and VEGF in the Induction of Angiogenesis in Vitro and Alters Endothelial Cell Extracellular Proteolytic Activity. *J. Cell. Physiol.* 1998, 177 (3), 439–452. DOI: 10.1002/(SICI)1097-4652(199812)177:3<439::AID-JCP7>3.0.CO;2-2.
- (40) van Nieuw Amerongen, G. P.; Koolwijk, P.; Versteilen, A.; van Hinsbergh, V. W. M. Involvement of RhoA/Rho Kinase Signaling in VEGF-Induced Endothelial Cell Migration and Angiogenesis in Vitro. *Arterioscler. Thromb. Vasc. Biol.* 2003, 23 (2), 211–217. DOI:10.1161/01.atv.0000054198.68894.88.
- (41) Fujimoto, A.; Onodera, H.; Mori, A.; Nagayama, S.; Yonenaga, Y.; Tachibana, T. Vasculogenic Mimicry and Mosaic Vessels in in Vivo and in Vitro Models of ECV304 Human Bladder Carcinoma Cells. *Cancer Res.* 2005, 65 (9 Supplement), 268–269. DOI: 10.1007/s00726-011-1214-6. Epub 2012 Jan 10.
- (42) Rundhaug, J. E. Matrix Metalloproteinases and Angiogenesis. *J. Cell. Mol. Med.* 2005, 9 (2), 267–285. DOI: 10.1111/j.1582-4934.2005.tb00355.x.
- (43) Sang, Q. X. Complex Role of Matrix Metalloproteinases in Angiogenesis. *Cell Res.* 1998, 8 (3), 171–177. DOI: 10.1038/cr.1998.17.
- (44) Kunz-Schughart, L. A.; Schroeder, J. A.; Wondrak, M.; van Rey, F.; Lehle, K.; Hofstaedter, F.; Wheatley, D. N. Potential of Fibroblasts to Regulate the Formation of Three-Dimensional Vessel-like Structures from Endothelial Cells in Vitro. *Am. J. Physiol. Cell Physiol.* 2006, 290 (5), C1385–C1398. DOI:10.1152/ajpcell.00248.2005.
- (45) Wenger, A.; Kowalewski, N.; Stahl, A.; Mehlhorn, A. T.; Schmal, H.; Stark, G. B.; Finkenzeller, G. Development and Characterization of a Spheroidal Coculture Model of Endothelial Cells and Fibroblasts for Improving Angiogenesis in Tissue Engineering. *Cells Tissues Organs* 2005, 181 (2), 80–88. DOI: 10.1159/000091097.
- (46) Fujimoto, A.; Onodera, H.; Mori, A.; Nagayama, S.; Yonenaga, Y.; Tachibana, T. Vasculogenic Mimicry and Mosaic Vessels in in Vivo and in Vitro Models of ECV304 Human Bladder Carcinoma Cells. *Cancer Res.* 2005, 65 (9 Supplement), 268–269. DOI: 10.1007/s00726-011-1214-6. Epub 2012 Jan 10.
- (47) Siemerink, M. J.; Klaassen, I.; Vogels, I. M. C.; Griffioen, A. W.; Van Noorden, C. J. F.; Schlingemann, R. O. CD34 Marks Angiogenic Tip Cells in Human Vascular Endothelial Cell Cultures. *Angiogenesis* 2012, 15 (1), 151–163. DOI:10.1007/s10456-011-9251-z. Epub 2012 Jan 17.

---

## Table of Contents artwork

